Advanced Composites and Hybrid Materials (2023) 6:3
https://doi.org/10.1007/s42114-022-00576-2

RESEARCH

Resveratrol-silica aerogel nanodrug complex system enhances the treatment of sports osteoarthritis by activating SIRT-1

Lili Qin[1] · Guoxin Jing[2] · Ningxin Cui[1] · Zhen Xu[1] · Yiwei He[1] · Yao Qin[1] · Tianfeng Lu[1] · Jingyu Sun[1] · Ai Du[3] · Shilong Wang[2]

Received: 7 July 2022 / Revised: 15 October 2022 / Accepted: 19 October 2022 / Published online: 2 December 2022

Abstract

Sports osteoarthritis (OA) is the most prevalent chronic joint disease in professional and recreational athletes. Resveratrol (RES), which is extracted from plants, has excellent anti-inflammatory properties. However, its application in OA treatment is limited by its poor water solubility, low bioavailability, and rapid metabolism. In this study, a silica aerogel (SA) was prepared through the sol–gel method and used to carry RES in the form of a nanodrug complex system (RSA) with a high drug–loading rate of 21.8% and a sustained release effect that lasted more than 6 hours. RSA had good biocompatibility in human chondrocytes when the concentration was less than 40 μg/mL and enhanced the anti-inflammatory actions of RES in vitro. A rat model of exercise-induced osteoarthritis was constructed to examine the therapeutic effects of RSA in vivo. Furthermore, the inflammatory factors involved in cartilage degradation and catabolism were reduced to 14.6–19.1% those of the original values after RES intervention, while the expression of type II collagen significantly increased. Moreover, RES was found to activate SIRT-1 by inhibiting the NF-κB-mediated inflammatory pathway, which also alleviated the degradation of cartilage matrix. These results indicated that the use of RSA could provide a novel noninvasive approach for targeted OA therapy with the potential for oral drug delivery.

Keywords Sports osteoarthritis · Silica aerogel · Resveratrol · Anti-inflammatory effect · Nanocarrier

1 Introduction

Sports osteoarthritis (OA) is a chronic degenerative disease with a high prevalence in active athletes, obese individuals, and elderly people and is responsible for decreasing their quality of life [1]. Inflammation of articular cartilage is considered a major feature of OA, which can cause pain, movement limitations, and disability, especially in professional athletes and sports participants [2]. Unfortunately, OA treatment strategies have always been a major challenge because few drugs can effectively control the development of inflammation and regenerate articular cartilage.

Oral drug administration is regarded as the most convenient and noninvasive therapy method. Therapeutic drugs for OA treatment mainly include nonsteroidal anti-inflammatory drugs (NSAIDs), such as ibuprofen and indomethacin [3, 4]. However, NSAIDs are only effective in the middle and later stages of OA and can lead to adverse gastrointestinal and cardiovascular reactions in OA patients [5, 6]. In addition, the intra-articular injection drugs, such as hyaluronic acid, can cause great pain to the patient during the treatment process (Table S1). Therefore, it is imperative to discover effective drugs that can relieve the pain experienced by patients and alleviate the development of OA. RES has a significant ability to promote anti-inflammatory effects and collagen formation, indicating its application prospects in relieving

Lili Qin and Guoxin Jing contributed equally to this article.

✉ Ai Du
duai@tongji.edu.cn

✉ Shilong Wang
wsl@tongji.edu.cn

[1] Department of Physical Education, Sports and Health Research Center, Tongji University, Shanghai 200092, People's Republic of China

[2] Research Center for Translational Medicine at East Hospital, School of Life Science and Technology, Tongji University, Shanghai 200092, People's Republic of China

[3] Shanghai Key Laboratory of Special Artificial Microstructure Materials and Technology, School of Physics Science and Engineering, Tongji University, Shanghai 200092, People's Republic of China

inflammation and pain [7, 8]. Despite its promising therapeutic applications, the bioavailability of RES is extremely low (less than 1%) [9] due to its photosensitivity [10], poor water solubility (only 0.03 g/L), and short plasma half-life. In recent years, drug delivery systems have provided an intelligent approach to boost the clinical application of RES. Various nanomaterials have been applied to support RES to optimize its performance on the treatment of osteoarthritis. Among them, scaffold materials based on cartilage tissue engineering have been studied the most, including natural or synthetic scaffold materials based on gelatin, collagen, hydrogel, etc. [11–13]. In addition, some studies have used liposomes and nanospheres to carry RES to explore their advantages and characteristics as drugs for in situ injection [14–16]. However, there is no report on the design of an oral nanomedicine to enhance the effectiveness of RES for OA treatment.

Preliminary studies by our research group found that nanocarriers can improve the stability and bioavailability of small molecule drugs, cytokines, and nucleic acid drugs to regulate inflammatory responses in the cellular or immune microenvironment [17–19]. However, it is difficult to carry RES with ordinary nanomaterials due to its high molecular weight. Aerogels are three-dimensional nanoporous materials with ultrahigh porosity that show numerous unique properties and advanced applications [20–22]. Recently, aerogels have been reported to have the potential to deliver various drugs [23]. Due to their variable physicochemical properties [24, 25], regulatable porous network structure and high-specific surface area capacity [26, 27], aerogels have better drug adsorption properties than traditional porous carrier materials, such as liposomes, emulsions, and polymeric nanoparticles. Among them, silica aerogels with advanced preparation methods are easily modified by manipulating the synthetic conditions. Furthermore, aerogels have emerged as one of the most exciting and promising carriers for drug delivery systems, owing to their great adsorption, high drug loading capacity, good biocompatibility, and sustained release effect [28, 29].

Our research group has long been devoted to the synthesis, modification, and properties of silica aerogels [30, 31]. In our previous study, a RES-loaded silica aerogel (RSA) was constructed as a system for sustained drug release. In this research, RES was loaded into a silica aerogel, and we demonstrated that the synthesis of these nanoparticles was achieved through the pore structure of the aerogel, which enhanced the sustained-release effect, decreased the biological cytotoxicity, and improved drug activity. The in vitro anti-inflammatory results indicated that RSA could inhibit the inflammatory response of chondrocytes. Furthermore, RSA notably mitigated the progression of OA in mice by enhancing SIRT-1 activation, which could suppress the NF-κB-mediated inflammatory pathway, thus alleviating the degradation of the cartilage matrix. In summary, this silica aerogel is a promising sustained-release platform for oral drug delivery that provides a potential strategy for sports osteoarthritis treatment (Scheme 1).

2 Results and discussion

2.1 Physicochemical properties of the drugs and materials

The silica aerogel was loaded with RES by the sol–gel method, and the 3D structural simulation image is shown in Fig. 1a. Detailed materials and methods have been shown in Supporting Information. RES exhibited clear geometric edges and sheet-like structures, which are common in cryo-pharmaceuticals (Fig. 1b). The SA exhibited a typical nanoporous structure with uniform and loosely arranged particles (Fig. 1c). Figure 1d shows that RES was encapsulated by the silica particles. The microstructure of RSA particles in this study was nanoscale in size, which differs from ordinary drug delivery system composites according to the diffusion-adsorption mechanism [32]. RES was coated on the SA, rather than adsorbed to its backbone. This structure protects the drug from external factors and maintains its stability.

The results in Fig. 1e and f indicated that both of the N_2 sorption isotherms of SA and RSA were type IV isotherms, a common characteristic of mesoporous materials. The pore sizes of SA and RSA were 8.10 nm and 9.45 nm, respectively, and both in the mesoporous range. The pore volume and specific surface area of the materials decreased significantly after drug loading, indicating that drug molecules were adsorbed into the pore channels, thus reducing the pore space and specific surface area (Table S2).

The structure of SA, RSA, and RES was detected using XRD patterns, FTIR, and Raman spectra. The results are shown in Fig. S1A–C, which indicated the RES in RSA might convert into amorphous form during the dissolution and phase separation processes. The samples were also tested by thermogravimetric analysis (see Fig. S1D for detail). According to Formula (1) in the Supporting Information (SI), it was calculated that the drug loading efficiency of RSA was 21.8% w/w, which is higher than the loading efficiency of other mesoporous silicon materials (~20% w/w) reported previously [33, 34] (detailed analysis is given in SI).

2.2 The RES release profile from RSA in vitro

The ability of RSA to enable sustained drug release was tested in simulated gastric juice and PBS with pH values of 2.0 and 7.4, respectively (Fig. S2A and B). More than 90% of the RES powder was rapidly released within 1 hr in both simulated gastric juice and PBS. The drug release curve increased almost linearly with a nearly constant release rate. Then, the

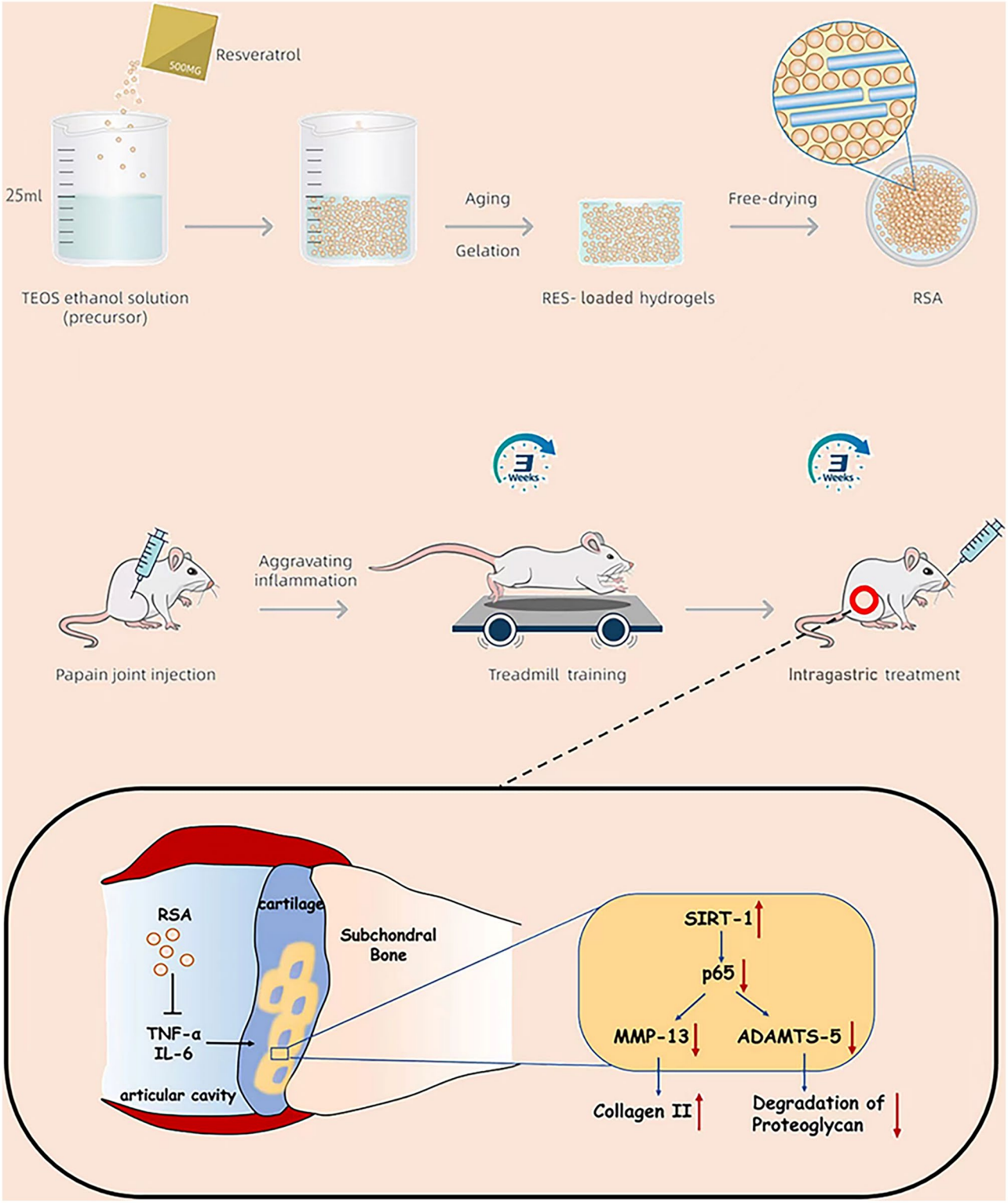

Scheme 1 Schematic diagram of the RSA preparation process and the regulatory mechanism of RSA in the treatment of sports osteoarthritis

concentration of released RES was basically unchanged from 1 to 3 hrs, indicating that RES was completely released into solution.

Drug release from RSA could be segmented into two stages. During the first stage, the concentration of released RES increased rapidly, and approximately 60% was released into

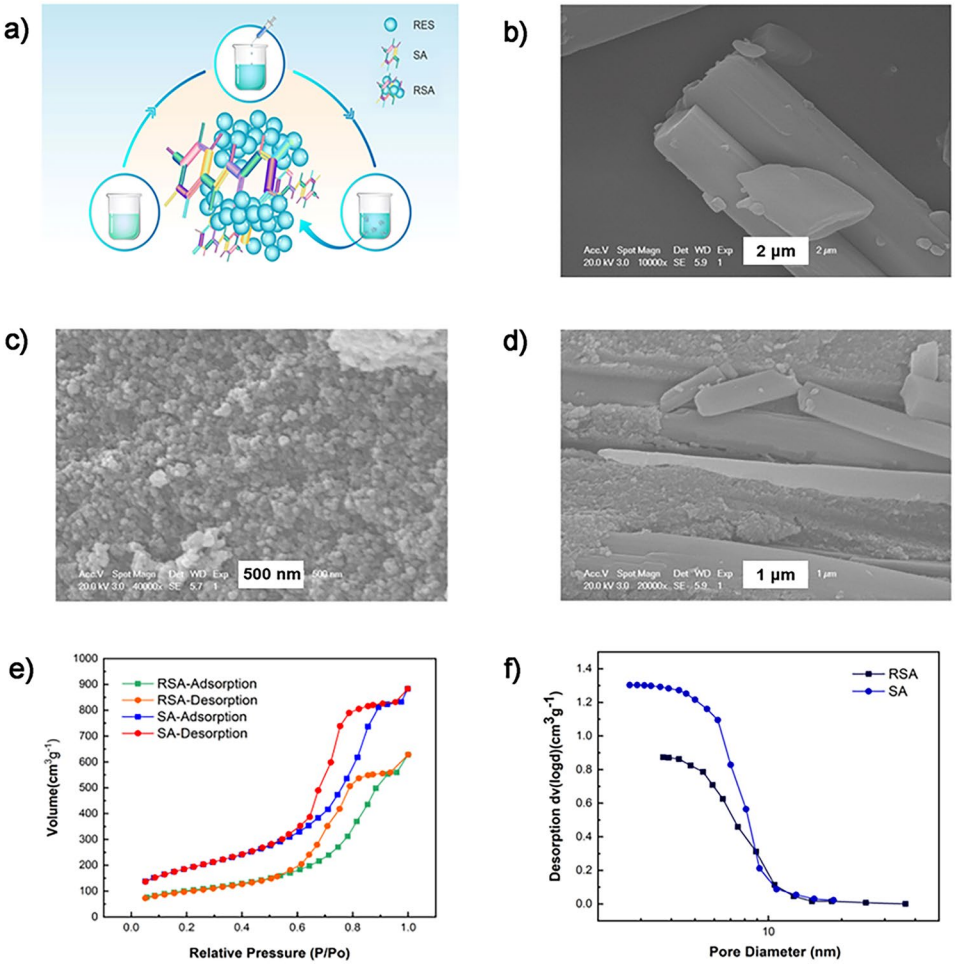

Fig. 1 Characterization of the materials and drugs. **a** Structural simulation image of RSA. **b** SEM image of RES. **c** SEM image of SA. **d** SEM image of RSA. **e** The isotherms of SA and RSA. **f** The pore size distributions of SA and RSA

solution within 30 min. The rate of RES release from RSA was higher than the release of free RES. The second stage of drug release began at 30 min and displayed a significantly slower rate than that of the first stage. The slope of each release curve decreased with time. The RES concentration rose sharply until it approached the theoretical maximum concentration, after which it remained stable for more than 6 hrs. The results above are consistent with our previous study, and the intrinsic mechanism underlying this effect is that the coating of SA could reduce the contact between active ingredients of pure drug and solution, which could reduce the release time of RES and invest a sustained release effect to RSA [35].

2.3 Cytotoxicity of RES, SA, and RSA to HC-A cells

To evaluate the biocompatibility of RES, SA, and RES, the in vitro cytotoxicity of these drugs was investigated in HC-A cells, a human chondrocyte cell line. The survival rates of the drug-treated chondrocytes were assessed by CCK-8 assay. As shown in Fig. 2a, after treatment with RES for 24 hrs, significant cytotoxicity was observed when the concentration was greater than 20 μg/mL. Moreover, after treatment with RES for 48 hrs and 72 hrs, the drug presented significant cytotoxicity at a concentration of 10 μg/mL. However, RSA exhibited better biocompatibility than RES. Chondrocytes treated with RSA exhibited decreased survival only when they were cocultured with RSA at concentrations greater than 60 μg/mL for 48 hrs or at concentrations greater than 40 μg/mL for 72 hrs. SA displayed good biocompatibility with chondrocytes at concentrations between 2.5 and 100 μg/mL. The proliferation rate of drug-treated chondrocytes was then evaluated via an EdU proliferation assay at concentrations between 2.5 and 40 μg/mL for 24 hrs (Fig. 2b and c). The fluorescence intensity of EdU was almost undetectable after treatment with RES when the RES concentration was greater than 20 μg/mL. However, SA and RSA showed no cytotoxicity at concentrations between 2.5 and 40 μg/mL, and the fluorescence of EdU hardly changed. The results above indicated that the cytotoxicity of RES could be significantly reduced when loaded into SA.

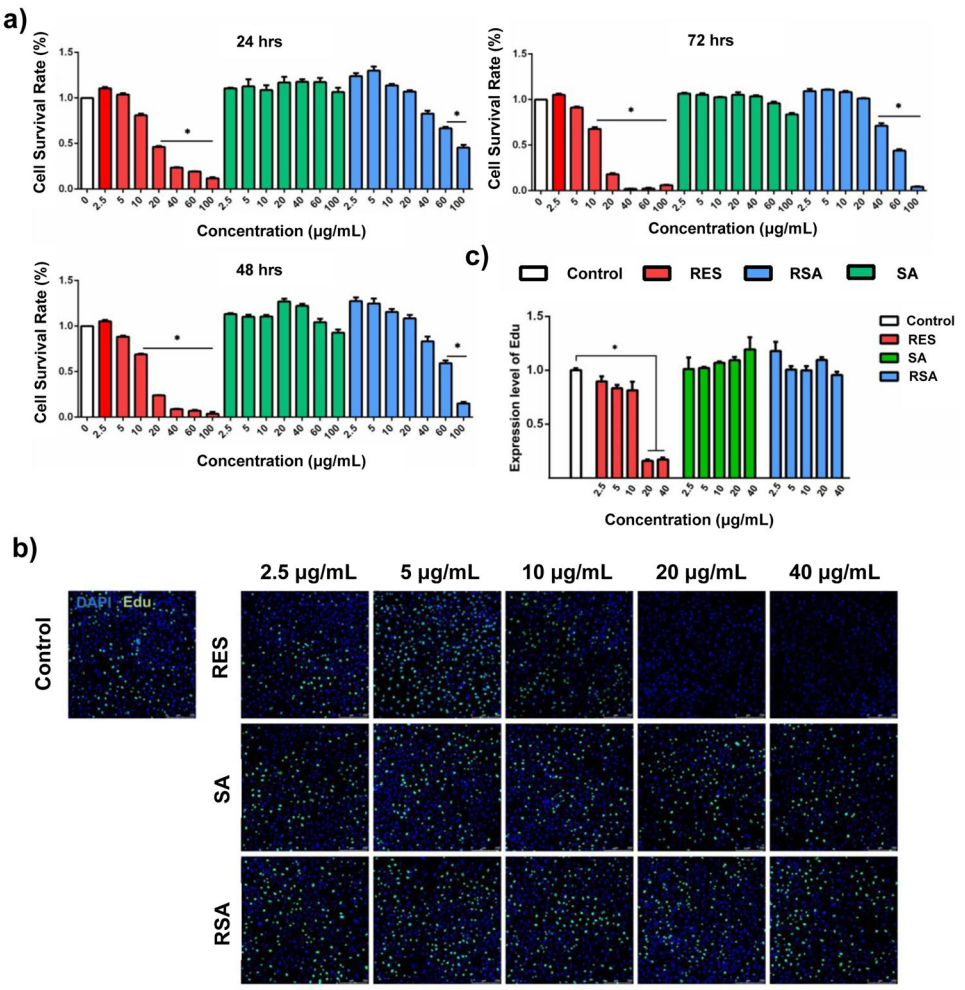

Fig. 2 Cytotoxicity of RES, SA, and RSA to HC-A cells. **a** CCK-8 analysis of HC-A cell viability after treatment with RES, SA, and RSA for 24, 48, and 72 hrs. All data are presented as the mean ± SEM ($n = 5$, single asterisk represents an average cell survival rate of less than 80%). **b** EdU assay of the proliferation of HC-A cells after treatment with RES, SA, and RSA for 24 hrs. Green fluorescence reflects the insertion of EdU, which represents HC-A cell proliferation. Nuclei were stained with DAPI (blue). Scale bars: 250 μm. **c** Quantification of the fluorescence in **b**. All data are presented as the mean ± SEM ($n = 3$, single asterisk represents average cell proliferation of less than 80%)

2.4 Anti-inflammatory effect of RSA in vitro

Inflammation is involved in the development and progression of osteoarthritis (OA) [36]. Secreted inflammatory molecules are critical mediators of inflammation in the pathophysiology of osteoarthritis, among which tumor necrosis factor (TNF) can drive the inflammatory cascade [37, 38]. In this research, lipopolysaccharide (LPS) was used to stimulate the inflammatory response in chondrocytes, and the expression of TNF-α was upregulated with increasing LPS concentration, which indicate the presence of an inflammatory response (Fig. 3a). The LPS-induced chondrocytes were then treated with RES, SA, and RSA. The results in Fig. 3b show that treatment with RSA reduced the expression of TNF-α to 27.1% of that in the blank group and was 1.7 times lower than that in the RES group. These results indicated that RSA could effectively inhibit the inflammatory response, and the effect was significantly better than that of RES. Previous research demonstrated that the inflammatory response can suppress anabolic activities in chondrocytes, which depress the synthesis of extracellular matrix (ECM) components, mainly collagen II and aggrecan. The results here indicated that RSA could alleviate the suppressed expression of collagen II and aggrecan under inflammatory conditions, and the effect was approximately 1.4 times better than that of RES (Fig. 3c). To further verify the results above, immunofluorescence staining was used to examine the expression of collagen II (Fig. 3d and e). LPS significantly inhibited the expression of collagen II, while treatment with RSA effectively relieved the restricted synthesis of collagen II, and the effect was enhanced with increasing RSA concentration. In addition, RSA performed better than RES. The results above suggest that RSA could enhance the anti-inflammatory ability of RES in vitro and has a significant effect on promoting the expression of ECM components in chondrocytes experiencing inflammation.

2.5 Cytotoxicity of RES, SA, and RSA in vivo

The blood biochemical indices of the rats in each group after intervention are listed in Table S4. The total amounts of albumin (ALB) and globulin (GLB) in the RSA-h, RSA-l,

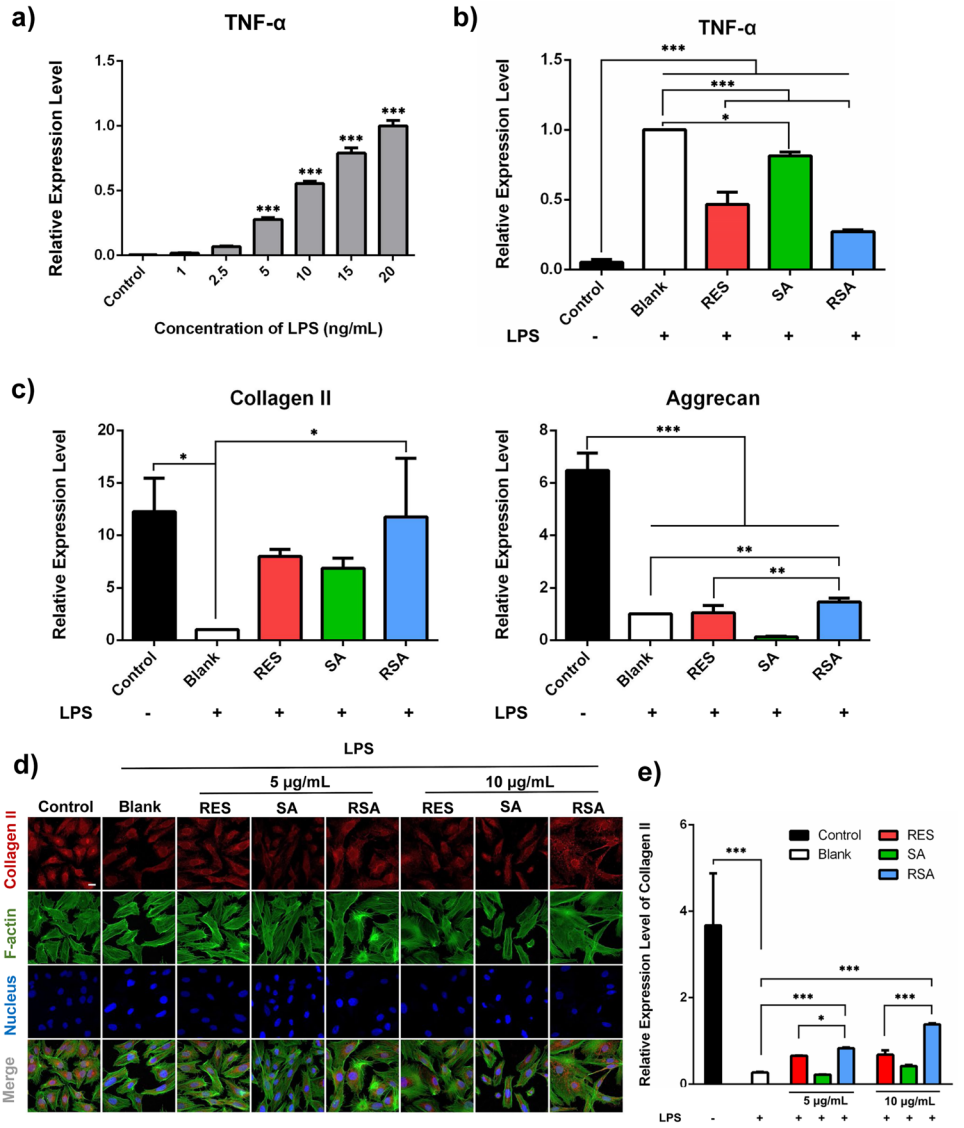

Fig. 3 In vitro protective effect of RSA in HA-C cells under inflammatory conditions. **a** The expression of TNF-α at the mRNA level after treatment with LPS at concentrations ranging from 0 to 20 ng/mL for 4 hrs. **b**, **c** RT−PCR reflecting the expression of TNF-α, collagen II, and aggrecan in HA-C cells after treatment with RES, SA, and RSA for 24 hrs and coculture with LPS for 3 hrs. The primer sequences are listed in Table S3, and *Gapdh* was used as the internal reference. **d** Immunostaining of HA-C cells after treatment with RES, SA, and RSA for 24 hrs and cocultured with LPS for 3 hrs. F-Actin was stained with FITC-labeled phalloidin (green), and nuclei were stained with DAPI (blue). Scale bars: 25 μm. **e** Quantification of the data in **d**. All data are presented as the mean ± SEM ($n=3$, $^{***}p<0.001$, $^{**}p<0.01$, $^{*}p<0.05$)

and RES groups were lower than that in the OA group in terms of the related indices of liver function. The white bulb ratios of the rats in the RSA-h, RSA-l, and RES groups were 0.86 ± 0.07, 0.88 ± 0.11, and 0.80 ± 0.11, respectively, after interventional treatment, all of which were within the normal range. There were no significant differences in total blood bilirubin (STB), alanine aminotransferase (ALT), aspartate aminotransferase (AST), or amylase (AMS) in the RSA-h, RSA-l, and RES groups compared with the control group. The urea (BUN) contents in the RSA-h, RSA-l, and RES groups were close to or even lower than those in normal rats and were significantly lower than those in the inflammatory group and blank control group ($p<0.05$). The triglyceride (TG) levels of the rats in the treated groups were significantly lower than those in the control group.

The weights of the rats were measured daily and recorded during the processes of modeling and drug intervention. The weight changes of the rats in each group are shown separately in Fig. 4a. The weights of the rats in all groups decreased from the 3rd week to the 4th week, which might be caused by exercise intervention. After the 5th week, the increases in body weight slowed down and gradually remained stable, which was consistent with the growth and development conditions of the SD rats. After modeling, the weights of the rats treated with RES were lower than those of the group not treated with RES.

2.6 The effect of RSA on OA in vivo

H&E staining was performed to examine the morphology of cartilage tissue (Fig. 4b). Compared with the OA group, the RSA-treated groups exhibit significantly reduced cracks in the cartilage matrix, a decrease in the number of proliferative cells, a continuous and relatively complete tidal line, and

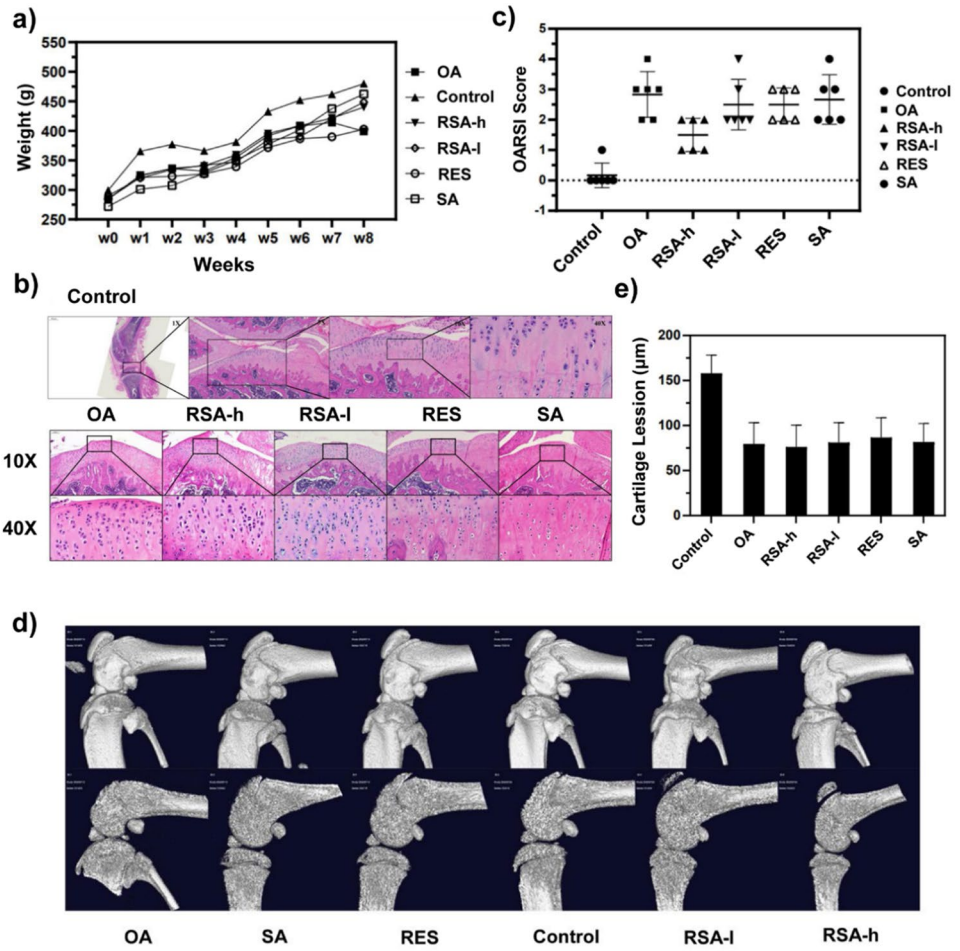

Fig. 4 The effect of RSA on OA in vivo. **a** The weights of the rats in each group throughout the whole experimental period. **b** H&E staining images of the weight-bearing areas on the medial edge of the tibial end of the knee cartilage in each group. **c** OARSI scores of articular cartilage. **d** Micro-CT images of the right knee joint in each group. **e** Right joint space

clear tissue on both sides. The healing effect increased with the concentration of drug, and loading by SA significantly improved drug efficacy. Mankin and OARSI scores were used to reflect subtle structural changes in the osteoarthritic tissue. The Mankin scores in Fig. 4c show a significant decrease after drug intervention compared to the inflammation group. The three drug intervention groups (RSA-h, RSA-l, and RES) showed lower Mankin scores. After intervention with the RES nanodrug carrier, compared with the OA group, the characteristics of joint inflammation were significantly reduced, and histological observation and OA score analysis further confirmed that the appearance of the cartilage surface was close to that of a normal joint. These results suggest that RES protected articular cartilage from damage in a dose-dependent manner.

In clinical trials, patients with knee osteoarthritis are usually evaluated by imaging to determine joint space width and osteophyte formation. In this experiment, a three-dimensional reconstruction model of the rat bone structure was obtained by in vivo imaging (Fig. 4d). In the control group, the knee joint spaces were normal, had no stenosis, smooth bone edges, and no osteophyte formation. In the other inflammatory model group, the CT images showed that the gap of the knee joint became narrow, the edge of the bone was rough, and osteophytes had formed. According to Fig. 4e, the joint space in the SD rats in the control group was 158.11 ± 20.12 ($n = 6$) before drug intervention, which was significantly different from that in the inflammatory group (234.17 ± 18.79, $n = 6$). After drug treatment, the joint space in each group was significantly reduced. Four weeks after drug intervention, the joint space in the three treatment groups (RSA-h, RSA-l, RES) was slightly reduced to 200.67 ± 17.69, 240.28 ± 21.49, and 220.98 ± 24.56, respectively. However, there was no significant difference between these three groups and the inflammatory group. According to these results, intervention with neither the pristine drug nor the nanodrug system could affect the subchondral bone structure, which indicated that short-term drug intervention could not change the bone structure fundamentally. The treatment of osteoarthritis is still a chronic and long-term process. If the time period of drug intervention is too short, it is difficult to improve the osteoarticular space without completely improving the cartilage matrix lesions.

2.7 Anti-inflammatory effect of RSA in vivo and the mechanism of this process

The expression of IL-6 is low in normal chondrocytes, whereas active inflammatory factors in osteoarthritis can stimulate its expression to increase [39, 40]. Figure 5a and b show the effects of RSA on the expression of the inflammatory cytokines IL-6 and TNF-α in chondrocytes. The expression levels of IL-6 and TNF-α in each inflammatory group were significantly upregulated compared with those in the control group. The expression levels of IL-6 and TNF-α in the RES, RSA-h, and RSA-l groups were significantly decreased compared with those in the OA group. The concentrations of IL-6 in the articular fluid of the RSA-l and RSA-h groups were 14.6% and 19.1% lower, respectively, than those in the RES group. The concentration of TNF-α in the RES group was significantly higher than that in the RSA-h group (16.5%), but no significant difference was observed between the RES and RSA-l groups. There were also no significant differences in the knee joint fluid inflammatory factors between the SA group and OA group. In addition, there were no significant differences in inflammatory factors in the left knee joint fluid in either the inflammatory group or the blank control group.

Proteoglycan (PG) is one of the most important components of articular cartilage and can enable cartilage tissue to bear the pressure load from the human body. PG degradation marks the beginning of cartilage degeneration in patients with OA [41, 42]. Figure 5c shows the content analysis of PG in each group of articular cartilage. Compared with the normal group, the PG expression level in the OA group was not abnormal, while the PG content in the RSA-h group was increased in both the left and right knee cartilage. Compared with the RSA-h group, the content of PG in the RSA-h group was significantly higher than that in the OA group in both the left knee and right knee. There was no significant difference in cartilage protein expression among the RSA-l, RES, and SA groups. These results showed that 4 weeks of RSA intervention significantly prevented PG degradation in the articular cartilage of OA model rats.

Sirtuin 1 (SIRT-1) is a negative regulator of inflammatory responses in vivo [43]. The SIRT-1 protein is expressed in the chondrocytes of all cartilage tissue layers [44]. A decrease in SIRT-1 can lead to an increase in apoptosis and activation of the NF-κB signaling pathway, which eventually causes an inflammatory response. p65 is a member of the NF-κB transcription factor family, and SIRT-1 is a direct target of p65 [45]. In addition, the secretion of inflammatory cytokines in the knee joint fluid can not only inhibit the expression of essential ECM components (e.g., aggrecan and collagen II) in chondrocytes but also induce the secretion of metalloproteinases by chondrocytes, such as collagenase MMP-13 (matrix

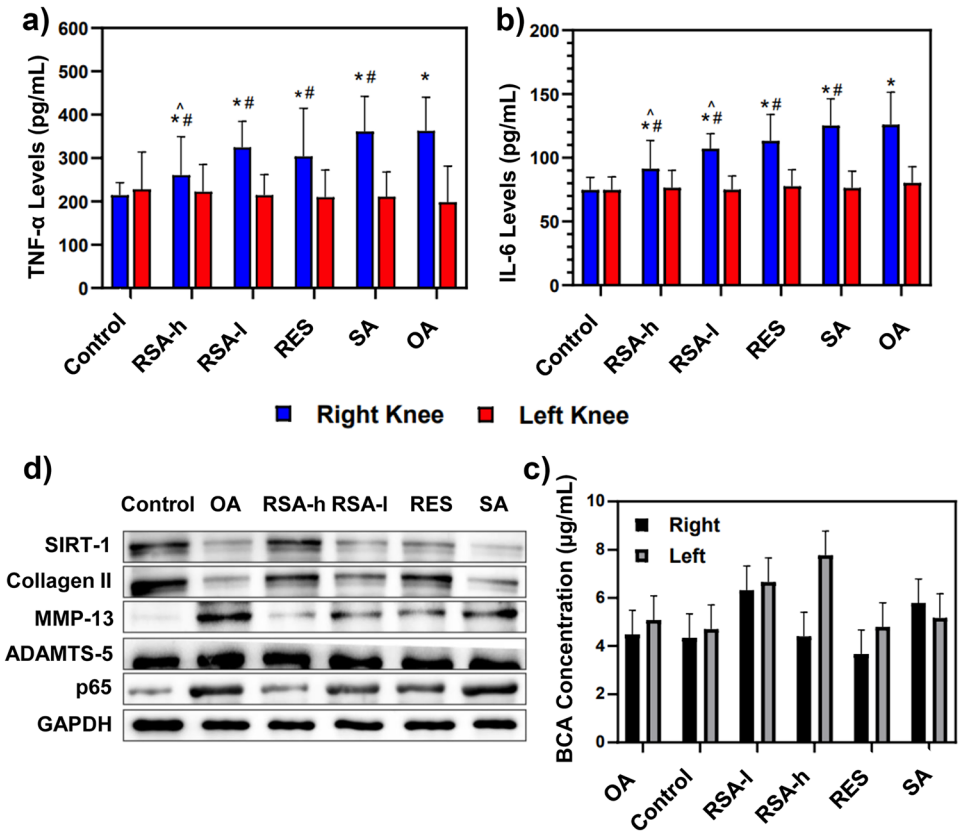

Fig. 5 Anti-inflammatory effect of RSA in vivo and the mechanism of this process. **a**, **b** Expression of TNF-α (**a**) and IL-6 (**b**) in articular cartilage (*Control group vs. OA RSA-h, RSA-l, RES, SA. # OA group vs. RSA-h, RSA-l, RES, SA. ^ RES group vs. RSA-h, RSA-l. *#^ $p < 0.05$). **c** Comparison of proteoglycan content in articular cartilage. **d** Western blot analysis of the expression of SIRT-1, collagen II, MMP-13 ADAMTS-5, and p65 in articular cartilage. GAPDH was used as a reference

metallopeptidase 13) and ADAMTS-5 (ADAM metallopeptidase with thrombospondin type 1 motif 5) [46]. Moreover, SIRT-1 can also inhibit the expression of cartilage-degrading enzymes such as ADAMTS-5 and MMP-13 by regulating the NF-κB pathway [47]. Therefore, we hypothesized that RSA might exert its anti-inflammatory effect by altering the expression of SIRT-1 to further inhibit the activation of the NF-κB signaling pathway. Herein, Western blotting was performed to detect the interactions between SIRT-1 and p65 and collagen II, MMP-13, and ADAMTS-5 (Fig. 5d). The expression of SIRT-1 in the cartilage tissue of the RSA-h group was significantly higher than that of the RES group and OA group ($p < 0.05$). Compared with that in the control group, the expression of the p65 protein in the OA group was significantly increased, and that in the RSA-h group was also increased. The expression of the p65 protein in the RSA-h group was significantly lower than that in the OA group and lower than that in the RSA-l and RES groups as well. The expression of p65 decreased and was similar to the level of p65 in the blank control group, which proved that RES exerted an inhibitory effect on NF-κB by activating SIRT-1. After low-dose RSA-1 intervention, the expression levels of SIRT-1 and p65 in chondrocytes were similar to those in the OA group without drug intervention, indicating that the activation of SIRT-1 by RES was dose-dependent. Furthermore, the expression of MMP-13 and ADAMTS-5 was consistent with that of SIRT-1 and opposite that of collagen II. These results confirmed the hypothesis that RSA possessed an excellent anti-inflammatory effect and could delay the degeneration of articular cartilage by inhibiting SIRT-1 and further suppressing the expression of the downstream NF-κB signaling pathway.

3 Conclusion

In this study, RSA was synthesized by the sol–gel method. The nanoparticles were incorporated into the pore structure of the aerogel, which improved drug activity and enhanced the sustained release effect. The in vitro results showed that RSA had excellent biocompatibility and cytotoxicity and could alleviate the progression of inflammation by regulating the expression of TNF-α, collagen II, and aggrecan in chondrocytes. Moreover, an in vivo study in OA model rats demonstrated that RSA could protect the cartilage matrix from degeneration and alleviate the development of OA by activating the SIRT-1-mediated inflammatory pathway. These results indicated that silica aerogels can serve as novel carriers for oral drug delivery and that RSA has potential application value for the noninvasive treatment of sports osteoarthritis.

Supplementary Information The online version contains supplementary material available at https://doi.org/10.1007/s42114-022-00576-2.

Author contribution L.Q., A.D, and S.W. provided the conception and design of the study. L.Q., N.C., and Y.H. completed the material synthesis and animal experiments. L.Q. and G.J. completed the in vitro experiments. L.Q., A.D., G.J., and N.C. co-wrote the main manuscript text. Z.X., Y.Q., T.L., and J.S. performed image and data analyses. All authors reviewed the manuscript.

Funding This work was funded by the National Key Research and Development Program of China (2017YFA0204600), the National Natural Science Foundation of China (Grant No. 31771313), and the China Postdoctoral Science Foundation (2021M692442).

Data availability Some or all data or models used during the study are available from the corresponding author by request.

Declarations

Competing interests The authors declare no competing interests.

References

1. Litwic A, Edwards MH, Dennison EM, Cooper C (2013) Epidemiology and burden of osteoarthritis. Br Med Bull 105(1):185–199. https://doi.org/10.1093/bmb/lds038
2. Malfait AM (2016) Osteoarthritis year in review 2015: biology. Osteoarthritis Cartilage 24(1):21–26. https://doi.org/10.1016/j.joca.2015.09.010
3. Wang KZ, Lei GH, Hu YC (2021) Chinese guideline for diagnosis and treatment of osteoarthritis. Chinese J Orthop 41(18):1291–1314. https://doi.org/10.3760/cma.j.cn121113-20210624-00424
4. Bannuru RR, Osani MC, Vaysbrot EE, Arden NK, Bennell K, Bierma-Zeinstra SMA, Kraus VB, Lohmander LS, Abbott JH, Bhandari M, Blanco FJ, Espinosa R, Haugen IK, Lin J, Mandl LA, Moilanen E, Nakamura N, Snyder-Mackler L, Trojian T, Underwood M, McAlindon TE (2019) OARSI guidelines for the non-surgical management of knee, hip, and polyarticular osteoarthritis. Osteoarthr Cartil 27(11):1578–1589. https://doi.org/10.1016/j.joca.2019.06.011
5. Persson MSM, Stocks J, Varadi G, Hashempur MH, Van Middelkoop M, Bierma-Zeinstra S, Walsh DA, Doherty M, Zhang W (2020) Predicting response to topical non-steroidal anti-inflammatory drugs in osteoarthritis: an individual patient data meta-analysis of randomized controlled trials. Rheumatol 59(9):2207–2216. https://doi.org/10.1093/rheumatology/keaa113
6. Lee AS, Ellman MB, Yan D, Kroin JS, Cole BJ, van Wijnen AJ, Im HJ (2013) A current review of molecular mechanisms regarding osteoarthritis and pain. Gene 527(2):440–447. https://doi.org/10.1016/j.gene.2013.05.069
7. Kang DG, Lee HJ, Lee CJ, Park JS (2018) Inhibition of the expression of matrix metalloproteinases in articular chondrocytes by resveratrol through affecting nuclear factor-kappa b signaling pathway. Biomol Ther 26(6):560–567. https://doi.org/10.4062/biomolther.2018.132
8. Collins JA, Moots RJ, Clegg PD, Milner PI (2015) Resveratrol and N-acetylcysteine influence redox balance in equine articular chondrocytes under acidic and very low oxygen conditions. Free Radic Biol Med 86:57–64. https://doi.org/10.1016/j.freeradbiomed.2015.05.008
9. Wenzel E, Somoza V (2005) Metabolism and bioavailability of trans-resveratrol. Mol Nutr Food Res 49(5):472–481. https://doi.org/10.1002/mnfr.200500010
10. Montsko G, Nikfardjam MSP, Szabo Z, Boddi K, Lorand T, Ohmacht R, Mark L (2008) Determination of products derived from trans-resveratrol UV photoisomerisation by means of HPLC-APCI-MS.

J Photochem Photobiol A Chem 196(1):44–50. https://doi.org/10.1016/j.jphotochem.2007.11.011
11. Wang W, Sun L, Zhang P, Song J, Liu W (2014) An anti-inflammatory cell-free collagen/resveratrol scaffold for repairing osteochondral defects in rabbits. Acta Biomater 10(12):4983–4995. https://doi.org/10.1016/j.actbio.2014.08.022
12. Choi SM, Lee KM, Ryu SB, Park YJ, Hwang YG, BaekD CY, Park KH, Park KD, Lee JW (2018) Enhanced articular cartilage regeneration with SIRT1-activated MSCs using gelatin-based hydrogel. Cell Death Dis 9(9):886. https://doi.org/10.1038/s41419-018-0914-1
13. Sheu SY, Chen WS, Sun JS, Lin FH, Wu T (2013) Biological characterization of oxidized hyaluronic acid/resveratrol hydrogel for cartilage tissue engineering. J Biomed Mater Res - Part A 101(12):3457–3466. https://doi.org/10.1002/jbm.a.34653
14. Wu G, Wang L, Li H, Ke Y, Yao Y (2016) Function of sustained released resveratrol on IL-1β-induced hBMSC MMP13 secretion inhibition and chondrogenic differentiation promotion. J Biomater Appl 30(7):930–939. https://doi.org/10.1177/0885328215614425
15. Kann B, Spengler C, Coradini K, Rigo LA, Bennink ML, Jacobs K, Offerhaus HL, Beck RCR, Windbergs M (2016) Intracellular delivery of poorly soluble polyphenols: elucidating the interplay of self-assembling nanocarriers and human chondrocytes. Anal Chem 88(14):7014–7022. https://doi.org/10.1021/acs.analchem.6b00199
16. Le Clanche S, Cheminel T, Rannou F, Bonnefont-Rousselot D, Borderie D, Charrueau C (2018) Use of resveratrol self-emulsifying systems in T/C28a2 cell line as beneficial effectors in cellular uptake and protection against oxidative stress-mediated death. Front Pharmacol. https://doi.org/10.3389/fphar.2018.00538
17. Wang J, Wang HY, Zhu RR, Liu Q, Fei J, Wang SL (2015) Anti-inflammatory activity of curcumin-loaded solid lipid nanoparticles in IL-1β transgenic mice subjected to the lipopolysaccharide-induced sepsis. Biomaterials 53:475–483. https://doi.org/10.1016/j.biomaterials.2015.02.116
18. Yang L, He XL, Jing GX, Wang H, Niu JH, Qian YC, Wang SL (2021) Layered double hydroxide nanoparticles with osteogenic effects as miRNA carriers to synergistically promote osteogenesis of MSCs. ACS Appl Mater Interfaces 13(41):48386–48402. https://doi.org/10.1021/acsami.1c14382
19. Zhu RR, Zhu XF, Zhu YJ, Wang ZJ, He XL, Wu ZR, Xue L, Fan WY, Huang RQ, Xu Z, Qi X, Xu W, Yu Y, Ren YL, Li C, Cheng Q, Ling L, Wang SL, Cheng LM (2021) Immunomodulatory layered double hydroxide nanoparticles enable neurogenesis by targeting transforming growth factor-β receptor 2. ACS Nano 15(2):2812–2830. https://doi.org/10.1021/acsnano.0c08727
20. Ji XJ, Zhong Y, Li CY, Chu JJ, Wang HQ, Xing Z, Niu TT, Zhang ZH, Du A (2021) Nanoporous carbon aerogels for laser-printed wearable sensors. ACS Appl Nano Mater 4(7):6796–6804. https://doi.org/10.1021/acsanm.1c00858
21. Ji XJ, Wang HQ, Chen TZ, Zhang T, Chu JJ, Du A (2020) Intrinsic negative TCR of superblack carbon aerogel films and their ultrabroad band response from UV to microwave. Carbon 161:590–598. https://doi.org/10.1016/j.carbon.2020.01.101
22. Yang JM, Cui NX, Han DX, Shen J, Wu GM, Zhang ZH, Qin LL, Zhou B, Du A (2021) A simple strategy for constructing hierarchical composite electrodes of PPy-posttreated 3D-printed carbon aerogel with ultrahigh areal capacitance over 8000 mF cm^{-2}. Adv Mater Technol 2101325. https://doi.org/10.1002/admt.202101325
23. Riley L, Schirmer L, Segura T (2019) Granular hydrogels: emergent properties of jammed hydrogel microparticles and their applications in tissue repair and regeneration. Curr Opin Biotechnol 60:1–8. https://doi.org/10.1016/j.copbio.2018.11.001
24. Xie PT, Sun W, Du A, Hou Q, Wu GM, Fan RH (2021) Epsilon-negative carbon aerogels with state transition from dielectric to degenerate semiconductor. Adv Electron Mater 7(3). https://doi.org/10.1002/aelm.202000877
25. Sun W, Du A, Feng Y, Shen J, Huang SM, Tang J, Zhou B (2016) Super black material from low-density carbon aerogels with subwavelength structures. ACS Nano 10(10):9123–9128. https://doi.org/10.1021/acsnano.6b02039
26. Xie PT, Sun W, Liu Y, Du A, Zhang ZD, Wu GM, Fan RH (2018) Carbon aerogels towards new candidates for double negative metamaterials of low density. Carbon 129:598–606. https://doi.org/10.1016/j.carbon.2017.12.009
27. Wu S, Du A, Huang SM, Sun W, Zu GQ, Xiang YL, Li CH, Zhou B (2016) Effects of monomer rigidity on the microstructures and properties of polyimide aerogels cross-linked with low cost aminosilane. RSC Adv 6(27):22868–22877. https://doi.org/10.1039/C5RA28152K
28. Du A, Zhou B, Zhang ZH, Shen J (2013) A special material or a new state of matter: a review and reconsideration of the aerogel. Materials 6(3):941–968. https://doi.org/10.3390/ma6030941
29. Stergar J, Maver U (2016) Review of aerogel-based materials in biomedical applications. J Sol-Gel Sci Technol 77(3):738–752. https://doi.org/10.1007/s10971-016-3968-5
30. Liu MF, Du A, Li TM, Zhang T, Zhang ZH, Cao GW, Li HW, Shen J, Zhou B (2019) Simple deceleration mechanism confirmed in the terminal hypervelocity impacted tracks in SiO_2 aerogel. Icarus 317:365–372. https://doi.org/10.1016/j.icarus.2018.08.017
31. Du A, Ma Y, Liu MF, Zhang ZH, Cao GW, Li HW, Wang L, Si PJ, Shen J, Zhou B (2021) Morphology analysis of tracks in the aerogels impacted by hypervelocity irregular particles. High Power Laser Sci and Eng 9(2):e14. https://doi.org/10.1017/hpl.2020.54
32. Alemán J, Chadwick AV, He J, Hess M, Horie K, Jones RG, Kratochvíl P, Meisel I, Mita I, Moad G, Penczek S, Stepto RFT (2007) Definitions of terms relating to the structure and processing of sols, gels, networks, and inorganic-organic hybrid materials (IUPAC Recommendations 2007). Pure Appl Chem 79(10):1801–1827. https://doi.org/10.1351/pac200779101801
33. Juère E, Florek J, Bouchoucha M, Jambhrunkar S, Wong KY, Popat A, Kleitz F (2017) In vitro dissolution, cellular membrane permeability, and anti-inflammatory response of resveratrol-encapsulated mesoporous silica nanoparticles. Mol Pharm 14(12):4431–4441. https://doi.org/10.1021/acs.molpharmaceut.7b00529
34. Summerlin N, Qu Z, Pujara N, Sheng Y, Jambhrunkar S, McGuckin M, Popat A (2016) Colloidal mesoporous silica nanoparticles enhance the biological activity of resveratrol. Colloid Surf B-Biointerfaces 144:1–7. https://doi.org/10.1016/j.colsurfb.2016.03.076
35. Qin LL, He YW, Zhao XY, Zhang T, Qin Y, Du A (2020) Preparation, characterization, and in vitro sustained release profile of resveratrol-loaded silica aerogel. Molecules 25(12):2752. https://doi.org/10.3390/molecules25122752
36. Kapoor M, Martel-Pelletier J, Lajeunesse D, Pelletier JP, Fahmi H (2011) Role of proinflammatory cytokines in the pathophysiology of osteoarthritis. Nat Rev Rheumatol 7(1):33–42. https://doi.org/10.1038/nrrheum.2010.196
37. Alaaeddine N, DiBattista JA, Pelletier JP, Cloutier JM, Kiansa K, Dupuis M, Martel-Pelletier J (1997) Osteoarthritic synovial fibroblasts possess an increased level of tumor necrosis factor-receptor 55 (TNF-R55) that mediates biological activation by TNF-alpha. J Rheumatol 24(10):1985–1994
38. Naume B, Shalaby R, Lesslauer W, Espevik T (1991) Involvement of the 55- and 75-kDa tumor necrosis factor receptors in the generation of lymphokine-activated killer cell activity and proliferation of natural killer cells. J Immunol 146(9):3045–3048
39. Guerne PA, Carson DA, Lotz M (1990) IL-6 production by human articular chondrocytes-modulation of its synthesis by cytokines, growth factors, and hormones in vitro. J Immunol 144(2):499–505
40. Bender S, Haubeck HD, Van de Leur E, Dufhues G, Schiel X, Lauwerijns J, Greiling H, Heinrich PC (1990) Interleukin-1β induces synthesis and secretion of interleukin-6 in human chondrocytes. FEBS Lett 263(2):321–324. https://doi.org/10.1016/0014-5793(90)81404-C

41. Setton LA, Elliott DM, Mow VC (1999) Altered mechanics of cartilage with osteoarthritis: human osteoarthritis and an experimental model of joint degeneration. Osteoarthritis Cartilage 7(1):2–14. https://doi.org/10.1053/joca.1998.0170
42. Mäkelä JTA, Han SK, Herzog W, Korhonen RK (2015) Very early osteoarthritis changes sensitively fluid flow properties of articular cartilage. J Biomech 48(12):3369–3376. https://doi.org/10.1016/j.jbiomech.2015.06.010
43. Li YS, Xiao WF, Wu P, Deng ZH, Zeng C, Li H, Yang TH, Lei G (2016) The expression of SIRT1 in articular cartilage of patients with knee osteoarthritis and its correlat. J Orthop Surg Res 11(1):144. https://doi.org/10.1186/s13018-016-0477-8
44. Yamamoto T, Miyaji N, Kataoka K, Nishida K, Nagai K, Kanzaki N, HoshinoY KR, Matsushita T (2021) Knee osteoarthritis progression is delayed in silent information regulator 2 ortholog 1 knock-in Mice. Int J Mol Sci 22(19):10689. https://doi.org/10.3390/ijms221910685
45. Kauppinen A, Suuronen T, Ojala J, Kaarniranta K, Salminen A (2013) Antagonistic crosstalk between NF-κB and SIRT1 in the regulation of inflammation and metabolic disorders. Cel Signal 25(10):1939–1948. https://doi.org/10.1016/j.cellsig.2013.06.007
46. Van den Berg WB (2011) Osteoarthritis year 2010 in review: pathomechanisms. Osteoarthr Cartil 19(4):338–341. https://doi.org/10.1016/j.joca.2011.01.022
47. Matsushita T, Sasaki H, Takayama K, Ishida K, Matsumoto T, Kubo S, Matsuzaki T, Nishida K, Kurosaka M, Kuroda R (2013) The overexpression of SIRT1 inhibited osteoarthritic gene expression changes induced by interleukin-1β in human chondrocytes. J Orthop Res 31(4):531–537. https://doi.org/10.1002/jor.22268